

GALAXY-SCALE CLOUDS OF IONIZED GAS AROUND AGN

S. DREW CHOJNOWSKI¹

Department of Physics and Astronomy, Texas Christian University, 76109

AND

WILLIAM C. KEEL

Department of Physics and Astronomy, University of Alabama, 35487

ABSTRACT

The serendipitous 2007 discovery of the object now known (even by NED) as ‘Hanny’s Voorwerp’ (Lintott et al. 2009) set into motion a search for more examples of galaxy-scale clouds of highly-ionized gas in the vicinity of active galactic nuclei (AGN). Using a sample assembled primarily by ‘citizen scientists’ via a dedicated thread in the Galaxy Zoo Forum, we carried out the first part of a larger long-slit spectroscopic survey of such objects with the 2.1m telescope at Kitt Peak National Observatory (KPNO). Of the 30 objects targeted during seven nights (multiple exposures for several), extended emission clouds were observed in 15 objects, with [OIII] λ 5007 emission occasionally extending >30 kpc from galaxy cores. A strong majority (11/15) of the extended emission clouds coincide with merging or otherwise violently disrupted systems, but more relevant to our search were the handful of clouds coinciding with isolated, symmetric galaxies lacking an obvious excitation mechanism. We present the results of part one in the hunt for Voorwerp analogues, much of which served to weed-out the more interesting objects to be targeted for future, multi-wavelength studies.

Subject headings: galaxies: active — galaxies: ISM — galaxies: individual: IC 2497 — galaxies: star formation

1. INTRODUCTION

The story of Hanny’s Voorwerp is a classic case of ‘Who done it?’ In the SDSS *gri* composite (see Fig.1), it appears as a ghostly blue, almost neon-blue, filament-like structure precariously located $\sim 15''$ south of the otherwise typical disc galaxy IC 2497. In their discussion of the Voorwerp as a possible ‘quasar light echo,’ Lintott et al showed that the object is gas-rich and so highly ionized that it appears to ‘see’ (or recently ‘saw’) an ionizing source which would resemble a quasar if it existed. While recent HST observations may help explain the true nature of the Voorwerp, possibly even identifying an energy source responsible for the observed level of ionization (does it even contain stars?), equally interesting would be an answer to the question of frequency. In other words, do Voorwerp analogues exist in the SDSS data?

Keeping with the mission of the Galaxy Zoo project, this was a question best answered by the thousands of dedicated ‘classifiers’ who continue to turn up strange objects long after the morphologies of the some 10^6 galaxies in the SDSS had already been classified. Scientific responses/explanations to such finds are made possible by an offshoot of the original project known as the Galaxy Zoo Forum. In April 2009, a thread was started in the Forum asking people to post galaxies with oddly colored filaments and/or loops, preferably in the vicinity of AGN (identified spectroscopically). These reports (100 pages worth as of today), in addition to those of a handful of ‘elite’ classifiers who perused images of ~ 16000 known AGN, produced a list of over 100 candidates.

The SDSS *gri* composite frame for Hanny’s Voorw-

erp and the IC 2497 ($z\sim 0.050$) system is shown in Fig.1 alongside the same for UGC 7342 ($z\sim 0.048$), and Mrk 463 ($z\sim 0.050$), the latter two of which are examples of objects pointed out by Galaxy Zoo classifiers as possible AGN clouds. Due to the coinciding redshifts, one can literally compare the physical scale of Voorwerp and ‘voorwerpje.’ Our goal in this survey was to do just that, though in far more detail, using information provided by long-slit spectra.

2. SAMPLE SELECTION

We examined in detail the *g* and *r* SDSS fields for each object in sample list. After subtracting average blank sky values from and aligning *g* and *r* frames, we scaled *r* frames to a value such that when subtracted from the *g* frame, all starlight was eliminated to the extent allowed by the *g-r* color gradients of stars within a given galaxy. In the case of IC 2497 and Hanny’s Voorwerp, all that remained in the frame following this process was the Voorwerp itself. The reason for this is that at the Voorwerp’s redshift, strong emission from [OIII] λ 4959, 5007 falls squarely into the *g* band and is thus mapped to blue in SDSS composites. Therefore, for objects at similar redshifts, we assumed that this ‘OIII filtering’ would produce similar results for true emission clouds, while simultaneously exposing false detections created by defects and/or misalignments in the SDSS *gri* composites.

Bright emission was confirmed around ~ 50 galaxies. For each such system, we used the SDSS images to derive position angles for long-slit spectroscopy. Aside from cases of multiple or faint nuclei, position angles were chosen in such a way that the slit would cover both galaxy nucleus and associated emission cloud.

Electronic address: drew.chojnowski@tcu.edu

¹ Southeastern Association for Research in Astronomy (SARA) NSF-REU Summer Intern

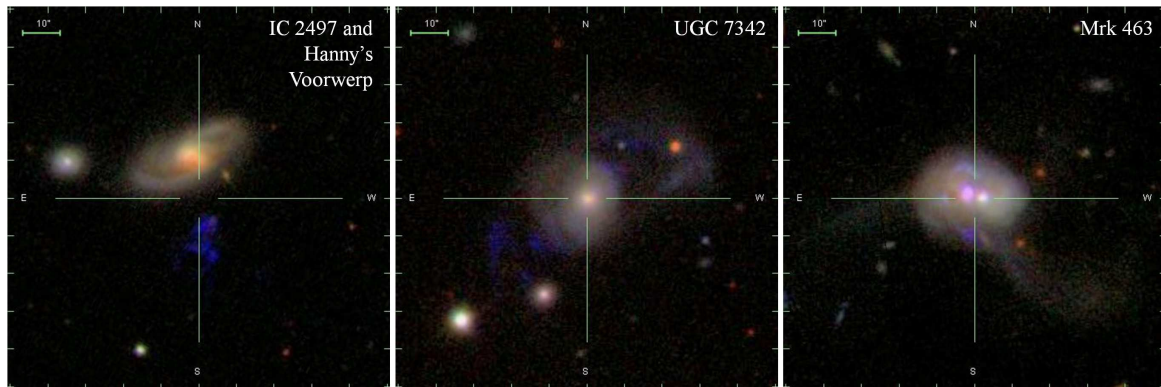


FIG. 1.— AGN cloud scale comparison

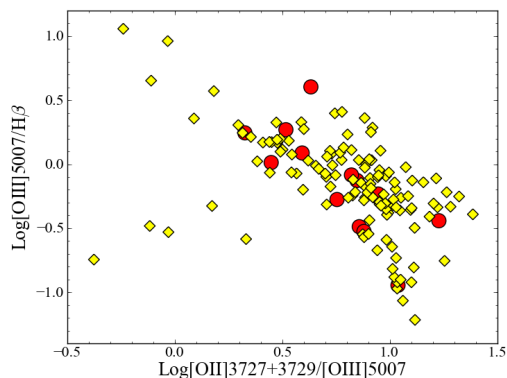


FIG. 2.— Diagnostic diagram for 12 KPNO targets. Red circles = target cores. Yellow diamonds = emission clouds. Core data points correspond to roughly 2 linear kpc, while emission cloud points correspond to 3 linear kpc intervals adjacent to target cores. Cloud points by target: UGC 7342 - 20, Mrk 298 - 15, Mrk 266 - 12, SDSS 1430+13 - 11, Mrk 1498 - 11, NGC 5972 - 11, Mrk 463 - 9, CGCG 428-014 - 8, Mrk 739 - 8, IC 2637 - 7, Mrk 273 - 7, Mrk 883 - 7, UGC 11185 - 7, SDSS 1510+07 - 7.

3. DATA AND REDUCTION

We used the GoldCam CCD spectrograph (GCam) on the 2.1m telescope at KPNO to obtain 45-min long-slit spectra for each of the 30 (out of 50) objects which were observable from early-summer Arizona. Spectra covered a range of 3300 - 5700 Å with noise becoming the dominant factor at wavelengths below $\approx 3500\text{Å}$. For objects showing strong emission, this range allowed us to capture high-ionization species such as $[\text{NeV}]\lambda\lambda 3346, 3426$ and $[\text{HeII}]\lambda 4686$ in addition to typically strong $[\text{OIII}]\lambda 5007$ and $\text{H}\beta$. Four spectacular examples of the latter are shown in Fig. 3. While there would have been obvious benefits to expanding spectral coverage into the red, doing so would have severely limited the number of targets observed. This was especially true considering that we chose to take the time to rotate the slit to a predetermined angle for each target. Not only does the telescope need to be at zenith for GCam rotation, an observer must manually rotate the instrument. While KPNO recommends that observers allow 10 minutes for each rotation, it can take longer when the platform beneath the telescope fails at precisely the second an intern lays a finger on the controls during the first-day walkthrough. The alternative to the platform is a rolling ladder and an observer taller than 6ft. We had one of each.

We used the 26new grating on GCam (2x300" long slit)

and the Ford 3K x 1K CCD (15 μm pixels). The pixel scale for GCam is 0.78"/pixel and the 26new grating disperses 1.24Å/pixel. With resolution around 2.7 Å, the $[\text{OII}]\lambda\lambda 3726$ and 3729 lines were rarely, if ever, resolved individually. A series of flat-field exposures were taken each evening, using the internal quartz lamp as a source, and were used to correct for instrumental eccentricities such as variation in pixel sensitivity. In addition, twilight flats were taken each evening in order to further improve pixel-to-pixel response and night-sky match. Series of HeNeAr lamp exposures were taken nightly to establish an overall wavelength fit, and single HeNeAr exposures were taken before or after each science exposure so that the effects of instrument flexure with changing position could be monitored.

We used standard IRAF procedures to reduce data. Bias, flat-field, and comparison lamp exposures were corrected for bias-levels in COLBIAS and combined with IMCOMBINE. All science frames were bias-subtracted, processed in COLBIAS, and divided by both a normalized flat-field and an illumination frame created from twilight flats via ILLUM. A wavelength scale was generated from the master HeNeAr frame using tasks IDENTIFY, REIDENTIFY, and FITCOORDS. The standard star Feige 34 was observed each night in order to generate a flux scale. The tasks APALL, STANDARD, and SENSFUNC were used for flux calibration. Wavelength and flux scales were applied to science frames by TRANSFORM and CALIB. Given that our target was often faint emission far from a continuum source, perhaps the most sensitive aspect to the reduction process was subtraction of background noise in BACKGROUND. Variations in wavelength scale due to instrument flexure, though minimal, were nonetheless eliminated by running SPLOT on comparison lamp frames adjacent to science frames. No attempt was made to remove cosmic rays.

4. ANALYSIS

4.1. Spectral Type

Emission line widths and ionization species were used to determine spectral types for the nuclei of each galaxy. Spectra with broad permitted lines were classified as Seyfert 1. Spectra with high-ionization lines but no broad component were classified as Seyfert 2. Intermediate spectra were assigned corresponding fractional Seyfert numbers while spectra with very weak high-ionization lines were called LINERS. Two starburst galaxies were observed and labeled HII. The most distant

TABLE 1
KPNO TARGET SUMMARY.

Object	SDSS ObjId	Redshift	Sy Type	Morph.	Scale of Cloud [kpc]
CGCG 077-117	588017703489372418	0.0371	2	S + tidal tail	19
CGCG 097-125	588023669168537695	0.0274	HII	?	-
CGCG 428-014	587727221400862869	0.0297	2	Tidal tails	18
IC 0812	587745544806727722	0.0145	HII	Assymmetric S	7
IC 2637	587734892748144649	0.0292	1.5	Asymmetric	17
IC 3929	588023670249750583	0.0807	2	Merger	-
KUG 1350+257	587739810484650051	0.0637	1.5	Merger	-
Mrk 266	587732483292266546	0.0279	2	Merger	31
Mrk 273	587735666377949228	0.0378	2	Merger	36
Mrk 298	587739720846934175	0.0342	LINER/HII	Tidal tails	60
Mrk 463	587742550676275314	0.0504	2	Merger	18
Mrk 739	587742013279502420	0.0299	1	Merger	17
Mrk 883	587736898503639075	0.0375	1.8	Merger	46
Mrk 1498	587736980102643827	0.0547	1.9	E	26
NGC 4388	588017566564155399	0.0084	2	Edge-on S	11
NGC 5252	587729158970736727	0.0230	1.5	S0	21
NGC 5675	587736583892238376	0.0133	LINER/HII	Tidal tails	-
NGC 5972	587739845390761994	0.0297	2	Tidal tails	35
SDSS J111100.60-005334.9	588848898833580220	0.0908	2	Merger	-
SDSS J142522.28+141126.5	587742609727684701	0.0598	2	Merger	-
SDSS J143029.88+133912.0	587736809916399664	0.0852	2	Asymmetric stellar loop	20
SDSS J151004.01+074037.1	588017991773520114	0.0458	2	S0	12
SDSS J151915.98+104847.8	587736813131989104	0.0988	1	SB0/a	-
SDSS J153508.93+221452.8	587739814240190581	0.0858	2	S + tidal tail	-
SDSS J153703.36+135944.1	587742590401904799	0.0737	LINER	Tidal tail	-
SDSS J210918.38-060754.7	587726879412256901	0.0288	2	SA	-
SDSS J214150.10+002209.4	587731186725683280	0.1074	2	S + tidal tail	-
UGC 07342	587739719750058064	0.0477	2	Sc (Merger?)	37
UGC 11185	758879745074397535	0.0412	2	Merger	11
VPC 0764	587732772131504164	0.1538	(2)	E multiple	-

NOTE. — Clouds scales are measured from galaxy nuclei to edge of emission. If emission extends in both directions from nuclei, the larger value is given. A dash indicates that the emission-line region was not spatially resolved.

galaxy observed was VPC 0764; we suspect it is a Seyfert 2 based on faint $[\text{OIII}]\lambda 5007$ and $\text{H}\beta$ detections.

The bulk of our sample host Seyfert 2 nuclei, possibly supporting the viewing angle explanation for the observed variety of AGN. Assuming validity of that explanation, viewing angle could have been a selection effect whereby ionized clouds around Seyfert 2 are simply more obvious in images. This idea is supported by the polar, jet-like velocity structure observed in clouds around systems such as Mrk 1498 and CGCG 428-014 (see Fig. 4).

4.2. Emission Line Diagnostics

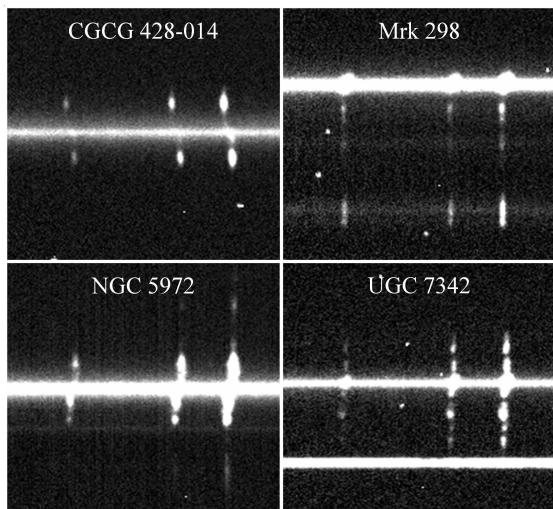


FIG. 3.— Snapshots of extended $\text{H}\beta/\text{OIII}$ emission.

Due to the distinct spectral shapes, blueward of the Lyman limit, of star-forming and AGN-ionized regions, diagnostic diagrams have long been recognized as an effective means for isolating star-forming spectra from those produced by a harder energy source (Baldwin et al. 1981). Typically these diagrams plot ratios of emission lines that are closely spaced, such as $[\text{NII}]\lambda 6583 / \text{H}\alpha$ versus $[\text{OIII}]\lambda 5007 / \text{H}\beta$, so as to sidestep the issue of reddening. Since our data covered only the blue half of the optical spectrum, we resorted to a less conventional form of the BPT diagram (Fig.2) where the ratio $[\text{OII}]\lambda\lambda 3727, 3729 / [\text{OIII}]\lambda 5007$ is plotted along the horizontal axis. All red points in the plot are ≈ 2 kpc line summations over the cores (peak flux) of twelve galaxies with confirmed AGN and extended emission clouds. The yellow points are 3 kpc intervals adjacent to cores, and while several clearly deviate from the main group, the point of the plot is to demonstrate that lines ratios similar to those measured around AGN cores were measured at large distances from cores as well.

4.3. Extent of Clouds

Linear extent estimates for emission clouds, summarized in Table 1, are based on extent of $[\text{OIII}]\lambda 5007$ emission. Object specific scale (Virgo infall only) numbers were pulled from NED. Readers of this paper are encouraged to look at the SDSS image for Mrk 298 if confirmation of the associated 60 kpc emission region (also see Fig.3) is desired. In this particular case, a more suitable description of the ionized cloud might be 'starburst jet.' High-ionization lines did not appear in the spectra of Mrk 298 or its cloud/jet. Such lines did appear in the spectra of UGC 7342 and its associated clouds, with

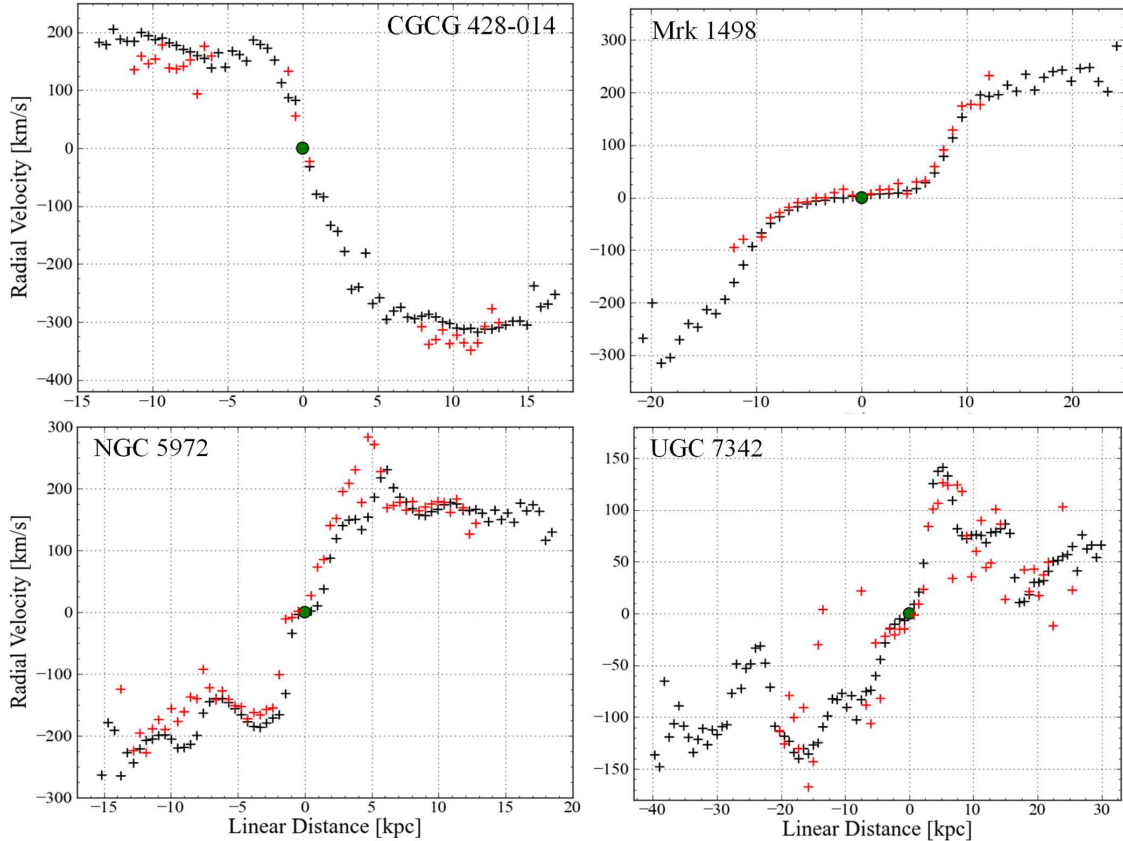


FIG. 4.— Emission cloud radial velocities relative to galaxy cores (green circles). Points represent line-by-line measurements of the [OIII] λ 5007 (black plus signs) and H β (red plus signs) emission lines.

[HeII] λ 4686 emission measurable for slightly more than 10 linear kpc in both directions adjacent to the galaxy core. The rather complex UGC 7342 emission structure is shown in Fig. 3 and mapped in Fig. 4.

5. DISCUSSION

5.1. Related Studies

While it appears that ours is the first survey of this class of objects, the literature contains a handful of relevant case studies beginning with a paper about Minkowskis Object by van Breugel et al. They found that a radio jet in NGC 541 was capable of inducing massive star formation in an HII region some 18 kpc from the jet source. Though sharing similar linear scales, Minkowskis Object and Hannys Voorwerp depart sharply in terms of level of excitation and therefore excitation mechanism. For example, where only very weak high-ionization lines were detected in the former, strong high-ionization lines were observed even at a linear distance of 22-31 kpc from the core of IC 2497 in the latter (Lintott et al. 2009). In terms of scale, our survey turned up several Voorwerp-sized clouds, most notably those associated with UGC 7342.

5.2. Binary AGN and Mergers

Several objects in our survey are well-documented in the literature due to binary AGN. The double Seyfert nuclei in Mrk 266 were discussed as early as 1980 by Petrosian et al, and in 1988, Hutchings et al noted remarkable structure in OIII line emission. Our data covered only one of the Seyfert nuclei, but our slit position

allowed us to capture the complex velocity structure apparent in [OIII] λ 5007 emission. Another binary AGN system, Mrk 463, was recently confirmed by Chandra, XMM-Newton, and HST data presented by Bianchi et al. Our slit was positioned over the brighter, eastern Seyfert 2 nucleus, where relatively strong NeV and HeII emission was detected. Another Markarian galaxy, Mrk 739, was discussed in 1987 by Netzer et al as a multiple nucleus galaxy. We confirm the Seyfert 1 nature of the brighter eastern nucleus and our data agree with the notion of an anisotropic central ionizing source which was mentioned in a Rafanelli et al study of merging Seyfert galaxies.

Violently disrupted systems were a recurring theme in this survey, with the majority of extended clouds corresponding with mergers or interactions. Particularly obvious cases include Mrk 883, UGC 11185, and Mrk273 (see SDSS images), the last of which is well-studied in the literature as home to the fourth OH megamaser ever discovered (Bottinelli et al. 1985).

5.3. Average = The New Extreme

Given the frequency of binary AGN and mergers among our sample, ‘average’ (narrow emission lines, relatively isolated and symmetric systems) galaxies hosting extended emission clouds were the more ‘extreme’ systems. Representative examples include SDSS 1510+07 and SDSS 1430+13. The most likely culprits in these cases are obscured AGN, so we turned to infrared data in search of evidence supporting re-radiation (by a dusty torus) in the far-IR of hard radiation produced in the

core.

By comparing far-IR data from IRAS, where available, to the ionizing luminosity 'seen' by the outermost emission cloud in a particular system, we can essentially 'balance the energy budget.' Where far-IR output matches implied ionizing luminosity, the budget is balanced and the case is closed as far as we are concerned. This appears to have been the case for several cloud hosts including NGC 4388, Mrk 273, and Mrk 883. Particularly intriguing, however, are multiple-factor mismatches between ionizing luminosity and far-IR. Of the 15 extended clouds observed, 7 fit this latter category, most notably SDSS 1430+13, where calculated ionizing luminosity at the outer edge of the cloud exceeds far-IR output around the core by a factor of 12. For NGC 5252, ionizing luminosity outweighs far-IR by a factor of 8, while for SDSS 1510+07, CGCG 428-014 and UGC 7342 the mismatch was a factor of ~ 3 . Wrapping up the list, with mismatches between ~ 1 -2, are NGC 5972 and UGC 11185.

Mysterious as the energy production deficits for certain galaxies may be, the fact that all ionized clouds surveyed are clearly linked to a host galaxy seemingly removes them from the Voorwerp analogue radar. On the other hand, the possibility remains that Hanny's Voorwerp is simply the most extreme case and that we should therefore not expect to find another.

6. CONCLUSIONS

We performed a spectroscopic survey of 30 objects in the SDSS which were visually identified by Galaxy Zoo

participants as potentially similar to Hanny's Voorwerp. Half of those objects show evidence of extended, occasionally galaxy-scale emission clouds which are clearly associated with a host galaxy. Two-thirds of that half can be explained as shocked or AGN-ionized gas clouds resulting either from merger events or from the violent conditions associated with galaxy cores containing binary Seyfert nuclei. The handful of systems defying these possibilities are believed to host highly obscured AGN whose energy output is apparently invisible even in the far-infrared. That being said, we must conclude that Hanny's Voorwerp remains every bit as unique as it was prior to our search efforts.

A few dozen more candidates remain on our list, and another survey is scheduled for this November on the Lick 3m. In addition, a Lick 3m follow-up of our KPNO survey has already been completed. Galaxy Zoo science team members used the Kast dual spectrograph to both extend spectral coverage into the red and acquire longer exposures for objects including Mrk 266, Mrk 883, Mrk 1498, NGC 5972, UGC 11185, SDSS 1430+13, and CGCG 428-014. Plans for x-ray and radio observations are being discussed in relation to the goals of shedding light on missing ionization sources and providing additional information on gas kinematics and cloud structure.

This project was funded by the National Science Foundation Research Experiences for Undergraduates (REU) program through grant NSF AST-1004872.

REFERENCES

- Baldwin, J. A., Phillips, M. M., & Terlevich, R. 1981, *PASP*, 93, 5
 Bianchi, S., Chiaberge, M., Piconcelli, E., Guainazzi, M., & Matt, G. 2008, *MNRAS*, 386, 105
 Bottinelli, L., Fraix-Burnet, D., Gouguenheim, L., Kazes, I., Le Squeren, A. M., Patey, I., Rickard, L. J., & Turner, B. E. 1985, *A&A*, 151, L7
 Hutchings, J. B., Neff, S. G., & van Gorkom, J. H. 1988, *AJ*, 96, 1227
 Lintott, C. J., et al. 2009, *MNRAS*, 399, 129
 Netzer, H., Kollatschny, W., & Fricke, K. J. 1987, *A&A*, 171, 41
 Petrosian, A. R., Saakian, K. A., & Khachikian, E. E. 1980, *Astrofizika*, 16, 621
 Rafanelli, P., Marziani, P., Birkle, K., & Thiele, U. 1993, *A&A*, 275, 451
 van Breugel, W., Filippenko, A. V., Heckman, T., & Miley, G. 1985, *ApJ*, 293, 83
 Wang, J.-B., & Gao, Y. 2010, *Research in Astronomy and Astrophysics*, 10, 309